The American Journal of Pathology, Vol. 180, No. 4, April 2012

DOI: 10.1016/j.ajpath.2011.12.016

Short Communication

Dorsal Root Ganglia Damage in SIV-Infected Rhesus Macaques

An Animal Model of HIV-Induced Sensory Neuropathy

Tricia H. Burdo,* Krystyna Orzechowski,* Heather L. Knight,† Andrew D. Miller,† and Kenneth Williams*

From the Department of Biology, Boston College, Chestnut Hill; and the Department of Comparative Pathology,† Harvard Medical School, New England Primate Research Center, Southborough, Massachusetts*

HIV-associated sensory neuropathy (HIV-SN) is currently the most common neurological complication of chronic HIV infection and continues to substantially affect patient quality of life. Mechanisms underlying the neuronal damage and loss observed in sensory ganglia of HIV-infected individuals have not been sufficiently studied. The present study aimed to develop and characterize a model of HIV-SN using SIV-infected CD8 T-lymphocyte-depleted rhesus macaques (*Macaca mulatta*). Uninfected controls ($n = 5$), SIV-infected CD8-depleted ($n = 4$), and SIV-infected non-CD8-depleted ($n = 6$) animals were used. Of the six non-CD8-depleted animals, three were conventional progressors (progressing to AIDS >1 year after infection) and three were rapid progressors (AIDS within 6 months). Dorsal root ganglia (DRG) were examined for histological hallmarks of HIV-SN, including satellitosis, presence of Nageotte nodules, and neuronophagia, as well as increased numbers of $CD68^+$ macrophages and abundant viral replication. In contrast to non-CD8-depleted animals, which had mild to moderate DRG pathology, the CD8-depleted SIV-infected animals had moderate to severe DRG damage, with increased numbers of $CD68^+$ satellite cells. Additionally, there was marked active viral replication in the affected DRG. These findings confirm that many features of HIV-SN can be recapitulated in the CD8-depleted SIV-infected rhesus macaque model within a short time frame and illustrate the importance of this model for study of sensory neuropathy. ***(Am J Pathol 2012, 180:1362–1369; DOI: 10.1016/j.ajpath.2011.12.016)***

Since the advent of antiretroviral therapy, many neurological complications resulting from HIV infection, including HIV-associated dementia, have declined.[1] Abnormalities of the peripheral nervous system (PNS), however, continue to be among the most common neurological complications of HIV-1 infection and are still poorly understood. Existing antiretroviral therapies have marginal effect on the incidence or severity of HIV-associated sensory neuropathy (HIV-SN),[2–8] and HIV-SN continues to substantially and negatively affect quality of life for chronically HIV-infected patients. The pathogenesis of non–drug-related toxicities in PNS disease remains to be elucidated. This quest has been hampered in the PNS by a lack of an appropriate model.

Rodents have generally been used as animal models for the study of nerve degeneration.[9,10] Although efficient in terms of relative ease of experimental manipulation, rodent models are comparatively poor models for lentiviral-associated sensory neuropathy. Feline immunodeficiency virus (FIV) infection, a lentiviral model of HIV in cats that causes marked immunosuppression, has been used occasionally to study the pathogenesis of sensory neuropathy.[5,11,12] Because of the evolutionary distance between rodents or cats and humans, nonhuman primates continue to be the most accepted and appropriate model of lentiviral pathogenesis.[13–18] Findings from a study using a model of pigtail macaques that were coinoculated with a neurovirulent cloned SIV virus (SIV/17E-Fr) and an immunosuppressive swarm virus (SIV/DeltaB670) showed development of multifocal trigeminal ganglionitis of varying severity, characterized by

Supported by a pilot grant from the Tulane National Primate Research Center (NIH P51-RR00164 to T.B.) and by NIH grants R01-NS40237 and R01-NS37654 (K.W.). The *in vivo* CD8-depletion antibodies used in these studies were provided by the NIH Nonhuman Primate Reagent Resource under grants RR016001 and AI040101.

Accepted for publication December 2, 2011.

Address reprint requests to Kenneth Williams, Ph.D., Department of Biology, Boston College, Higgins Hall 468, 140 Commonwealth Avenue, Chestnut Hill, MA 02467. E-mail: kenneth.williams.3@bc.edu.

multifocal mononuclear infiltrates, neuronophagia, and neuronal loss.[19]

In the present study, we used a CD8 T-lymphocyte-depleted (hereafter, CD8-depleted) SIV-infected rhesus macaque model, which results in the rapid onset of SIV-associated disease; >77% of persistently (>28 days) depleted macaques develop SIV encephalitis, with a progression to terminal AIDS within 12 weeks after infection. This model is highly reproducible and is commonly used to investigate monocyte/macrophage activation and traffic, peripheral immune responses, and central nervous system (CNS) disease.[20–28] This model has not previously been examined as a potential model for HIV-SN. Given the similarities between HIV infection and CNS disease and SIV encephalitis, we hypothesized that this rapid model might also be useful for a model of HIV-SN in humans. The present study aimed to develop a model of HIV-SN using SIV-infected CD8-depleted rhesus macaques, to aid in understanding of the pathogenic mechanisms underlying development of HIV-SN.

Materials and Methods

Animals, Viral Infection, and CD8 Lymphocyte Depletion

Five cohorts of rhesus macaques (*Macaca mulatta*) were used, a total of 15 animals. The first cohort (uninfected, CD8-depleted; M1 and M2) consisted of two uninfected control animals that were CD8-depleted by treatment with a human anti-CD8 antibody administered only once (50 mg/kg i.v.). The human anti-CD8 antibody was provided by the NIH Nonhuman Primate Reagent Resource.[14–17,26,28] The second cohort consisted of three uninfected non-CD8-depleted control animals (uninfected, non-CD8-depleted; M3 to M5). The third cohort (CD8-depleted; M6 to M9) consisted of four animals that were inoculated with a viral swarm SIVmac251 (a generous gift from Ronald Desrosiers, New England Primate Research Center, Southborough, MA) and were treated with human anti-CD8 antibody cM-T807 to achieve rapid disease progression with a high incidence of SIV encephalitis. These animals were administered 10 mg/kg s.c. of anti-CD8 antibody at day 6 after infection and 5 mg/kg i.v. at days 8 and 12 after infection. In the CD8-depleted groups, animals were defined as persistently depleted if the CD8 cells were depleted for >28 days. In the present study, all of the animals were persistently depleted, and CD8 levels were partially recovered at the time of necropsy in all animals except M9. Cohort 4 (non-CD8-depleted, rapid progressors; M10 to M12) consisted of three SIV-infected animals that were not CD8-depleted and that developed AIDS within 6 months after infection. Cohort 5 (non-CD8-depleted, conventional progressors; M13 to M15) consisted of three SIV-infected animals that were not CD8-depleted and that developed AIDS ≥1 year after infection.

To compare only peripheral effects of SIV infection, animals were selected that developed SIV encephalitis, as defined by the presence of multinucleated giant cells and accumulation of parenchymal and perivascular infiltrates of macrophages in the brain.[15,16,18,29] All animals were anesthetized with ketamine HCl, euthanized by an intravenous pentobarbital overdose, and exsanguinated. Animals from cohorts 1 and 3 were housed at the New England Primate Research Center (Southborough, MA) and animals from cohorts 2, 4, and 5 were housed at Tulane University's National Primate Research Center (Covington, LA) in strict accordance with standards of the American Association for Accreditation of Laboratory Animal Care.

Necropsy and Histopathology

Animals were necropsied immediately after death. Representative sections of all major organs were collected, fixed in 10% neutral buffered formalin, embedded in paraffin, sectioned at 5 μm, and stained using H&E. Staining was performed as follows. Tissues were deparaffinized in xylene, hydrated in graded alcohols, counterstained with Harris hematoxylin solution (Sigma-Aldrich, St. Louis, MO) for 2 minutes, and rinsed with running water. The slides were then dipped sequentially in acid alcohol (90% methanol, 5% sulfuric acid, 5% acetic acid; Sigma-Aldrich) and ammonia water (15 to 20 drops ammonium hydroxide in 250 mL water; Sigma-Aldrich), with a rinse under running water after each dip, followed by 80% alcohol for 2 minutes and then eosin (Sigma-Aldrich) for 2 minutes. Finally, tissue sections were rinsed in graded alcohols, dehydrated with xylene, and mounted with Vecta-Mount medium (Vector Laboratories, Burlingame, CA).

Histopathological Analysis of Dorsal Root Ganglia Morphology

H&E-stained sections of dorsal root ganglia (DRG) were evaluated blindly for histopathological lesions by a board-certified pathologist (A.D.M.); scoring was based on the presence and severity of infiltrating mononuclear cells, neuronophagia, and neuronal loss/degeneration. Ganglionitis was scored as 1, 2, or 3 according to the following criteria: mild (1), for scattered infiltrating mononuclear cells with rare evidence of neuronophagia and/or neuronal loss; moderate (2), for increased numbers of infiltrating mononuclear cells with occasional neuronophagia and/or neuronal loss; and severe (3), for abundant infiltrating mononuclear cells, frequent neuronophagia, and neuronal loss.

Immunohistochemistry

DRG sections were deparaffinized with xylene, hydrated in a series of graded alcohols, and stained with a pan-macrophage marker anti-CD68 (Dako, Carpinteria, CA), anti-SIV protein p28 (Bartels; Trinity Biotech USA, Jamestown, NY), a pan-T-cell marker anti-CD3 (Dako) or anti-CD8 (Vector Laboratories). Sections were counterstained with hematoxylin, dehydrated, and mounted using Vecta-Mount permanent mounting medium (Vector Laboratories). Sections were visualized and photographs taken

Table 1. Animals Used in Developing an Rhesus Macaque Model of HIV-Induced Sensory Neuropathy

Cohort and animal ID	Survival (months)	DRG pathology	CD68$^+$		SIV p28$^+$	
			%	cells/mm^2	%	cells/mm^2
Cohort 1: uninfected, CD8-depleted						
M1	NA	None	13.8 ± 0.01	491.5 ± 20.9	NA	NA
M2	NA	None	11.6 ± 0.007	683.2 ± 74.1	NA	NA
Cohort 2: uninfected, non-CD8-depleted						
M3	NA	None	15.4 ± 0.8	569.7 ± 24.0	NA	NA
M4	NA	None	15.3 ± 0.6	528.9 ± 107.2	NA	NA
M5	NA	None	11.8 ± 1.2	420.6 ± 64.1	NA	NA
Cohort 3: SIV-infected, CD8-depleted						
M6	2.6	Severe	28.1 ± 1.9	1342.0 ± 146.9	8.2 ± 1.4	317.4 ± 51.6
M7	4.4	Moderate-severe	26.1 ± 1.8	1338.3 ± 72.0	5.0 ± 0.7	216.1 ± 36.7
M8	3.0	Moderate-severe	25.3 ± 0.7	1292.0 ± 50.8	1.5 ± 0.2	66.8 ± 11.5
M9	2.0	Moderate	19.1 ± 1.1	814.5 ± 72.0	1.2 ± 0.3	60.1 ± 15.8
Cohort 4: SIV-infected, non-CD8-depleted, rapid progressors						
M10	3.9	Mild-moderate	38.0 ± 1.6	1820.9 ± 65.8	4.8 ± 0.8	143.5 ± 49.4
M11	5.1	Mild-moderate	27.3 ± 3.2	1148.3 ± 231.5	45.6 ± 1.3	1921.8 ± 225.9
M12	2.0	Mild	16.1 ± 0.8	663.1 ± 56.8	10.5 ± 3.2	432.1 ± 131.4
Cohort 5: SIV-infected, non-CD8-depleted, conventional progressors						
M13	19.0	Mild-moderate	24.5 ± 1.2	1095.0 ± 86.4	2.0 ± 0.3	70.3 ± 7.4
M14	17.7	Mild	19.6 ± 1.4	833.6 ± 60.2	2.0 ± 0.2	70.0 ± 9.2
M15	14.2	Mild	10.6 ± 0.3	560.8 ± 45.4	2.6 ± 0.1	127.1 ± 18.8

(*table continues*)

Data are expressed as means ± SEM. The percentage of positive cells was calculated as the number of positively stained cells divided by the total number of satellite cells (total hematoxylin-positive cells) surrounding the DRGs, multiplied by 100. Eight 20× fields were used for each measurement. The absolute number of cells was calculated as the cells/mm^2 in eight separate 0.147-mm^2 fields by dividing the number of positive cells in the field by the size of the field examined (eg, for a 20× field, it was 0.147 mm^2).

NA, not applicable.

using a Zeiss Axio Imager M1 microscope (Carl Zeiss MicroImaging, Thornwood, NY) with Plan-Apochromat 20×/0.8 and 40×/0.95 Korr objectives. The number of CD68$^+$, viral p28$^+$, CD3$^+$, and CD8$^+$ cells were counted manually. Data are expressed as a percentage of total satellite cells, calculated by dividing the number of positively stained cells by the total number of cells stained with hematoxylin and multiplying by 100. The absolute number of cells (positive cells/mm^2) was calculated by dividing the number of positive cells in the field by the size of the field examined (each 20× field was 0.147 mm^2). Cell counts were performed on eight nonoverlapping fields per DRG tissue section per animal at ×200 magnification.

Bromodeoxyuridine Administration

Bromodeoxyuridine (5-bromo-2′-deoxyuridine; BrdU) was administered 24 hours before necropsy as a slow bolus injection (60 mg BrdU/kg body weight, i.v.).

Results

Histopathology

Two uninfected CD8-depleted (cohort 1), three uninfected non-CD8-depleted (cohort 2), four SIV-infected CD8-depleted (cohort 3), and six SIV-infected non-CD8-depleted rhesus macaques (cohorts 4 and 5) were used in the present study (Table 1). Of the six SIV-infected non-CD8-depleted animals, three were rapid progressors (AIDS progression within 6 months) (non-CD8 depleted: rapid progressors) and three were conventional progressors (progressed to AIDS >1 year after infection) (non-CD8 depleted: conventional progressors) (Table 1). DRG tissue sections from uninfected controls had healthy neurons surrounded by a thin layer of supportive satellite cells (Figure 1A), regardless of CD8 T-cell depletion status. DRG from all CD8-depleted SIV-infected animals revealed variable satellitosis, neuronophagia, and development of Nageotte nodules, which are compact areas of satellite cells that accompany DRG neuronal loss (Figure 1B). Morphological assessment of DRG from non-CD8-depleted infected macaques demonstrated less severe peripheral neuropathy than that found in CD8-depleted macaques, with three animals having mild lesions and three animals having mild to moderate DRG pathology (Table 1). The DRG pathology was similar in nondepleted SIV-infected animals regardless of whether they were rapid or conventional progressors (Figure 1, C and D).

Immunohistochemistry

To characterize the degree of satellitosis and neuronophagia in the CD8-depleted SIV-infected animals, sections of DRG tissues were immunostained with an anti-CD68 monoclonal antibody (Figure 2). In uninfected CD8-depleted macaques, CD68 immunostaining identified a resident population of CD68$^+$ macrophages diffusely scattered around the DRG neurons (Figure 2A). In

Table 1. *Continued*

CD3$^+$		CD8$^+$		Cells per DRG neuron (no.)
%	cells/mm^2	%	cells/mm^2	
2.6 ± 0.7	101.1 ± 24.0	4.6 ± 1.0	165.0 ± 28.1	13.8 ± 0.7
6.4 ± 0.7	191.2 ± 21.1	2.0 ± 0.3	68.3 ± 9.7	12.7 ± 0.6
11.2 ± 1.2	597.6 ± 62.8	10.7 ± 0.7	236.9 ± 19.5	12.4 ± 0.6
7.0 ± 0.5	293.5 ± 26.6	4.6 ± 0.4	134.7 ± 12.8	10.3 ± 0.8
8.2 ± 0.8	345.4 ± 27.8	8.4 ± 0.7	255.9 ± 26.7	12.3 ± 0.5
7.6 ± 1.4	252.6 ± 36.0	1.7 ± 0.3	57.3 ± 11.8	26.9 ± 1.2
3.6 ± 0.4	134.4 ± 15.4	1.0 ± 0.2	29.9 ± 6.5	23.1 ± 1.5
3.1 ± 0.4	122.6 ± 8.9	6.2 ± 0.7	200.8 ± 28.4	12.9 ± 0.4
1.7 ± 0.5	96.3 ± 23.3	0.0 ± 0.0	0.0 ± 0.0	14.8 ± 0.7
5.7 ± 0.5	266.0 ± 22.7	6.7 ± 0.7	212.0 ± 13.0	11.5 ± 0.7
4.4 ± 0.9	152.3 ± 30.3	2.4 ± 0.7	88.8 ± 17.1	18.7 ± 1.8
3.0 ± 0.3	123.3 ± 14.8	0.0 ± 0.0	0.0 ± 0.0	13.3 ± 0.9
12.1 ± 1.8	513.6 ± 45.2	17.8 ± 2.1	574.2 ± 34.2.	13.2 ± 0.7
5.3 ± 0.6	243.2 ± 23.7	5.1 ± 0.1	253.5 ± 6.8	15.3 ± 1.0
19.3 ± 4.0	778.0 ± 85.7	13.0 ± 0.4	589.9 ± 17.5	11.6 ± 0.6

the two CD8-depleted controls, 13.8% and 11.6% of the total satellite cells were CD68$^+$ (491.5 and 683.2 CD68$^+$ satellite cells/mm^2 of tissue, respectively) (Table 1 and Figure 2A). Immunostaining for CD68 in DRG of the CD8-depleted SIV-infected macaques revealed a significant 1.5-fold to 2.0-fold increase in CD68$^+$ cells, compared with uninfected controls ($P < 0.05$, unpaired *t*-test) (Table 1). The quantity of CD68$^+$ cells in DRG tissue from CD8-depleted SIV-infected animals ranged from 814.5 to 1342.0 cells/mm^2. Activated CD68$^+$ macrophages (based on IHC and morphology) in the CD8-depleted SIV-infected animals had more prominent cell processes, compared with control

Figure 1. H&E staining of DRG tissues reveals neuronophagia and inflammatory infiltrates in CD8-depleted SIV-infected rhesus macaques. **A:** A representative DRG tissue section from an uninfected rhesus macaque (M1) demonstrates healthy neurons surrounded by a thin layer of supportive satellite cells. **B:** A representative section of DRG tissue from a CD8-depleted SIV-infected rhesus macaque (M8) reveals satellitosis, neuronophagia, and the development of Nageotte nodules (**arrow**). **C:** Representative section of DRG tissue from a non-CD8-depleted SIV-infected rapid progressor rhesus macaque (M11) that progressed to AIDS within 6 months. Representative neuronophagia is indicated by an **arrow**. **D.** Representative section of DRG tissue from a non-CD8-depleted SIV-infected rhesus macaque that was a conventional progressor (M15). The DRG pathology is similar in nondepleted SIV-infected animals, regardless of whether they were rapid or conventional progressors. Scale bars: 100 μm.

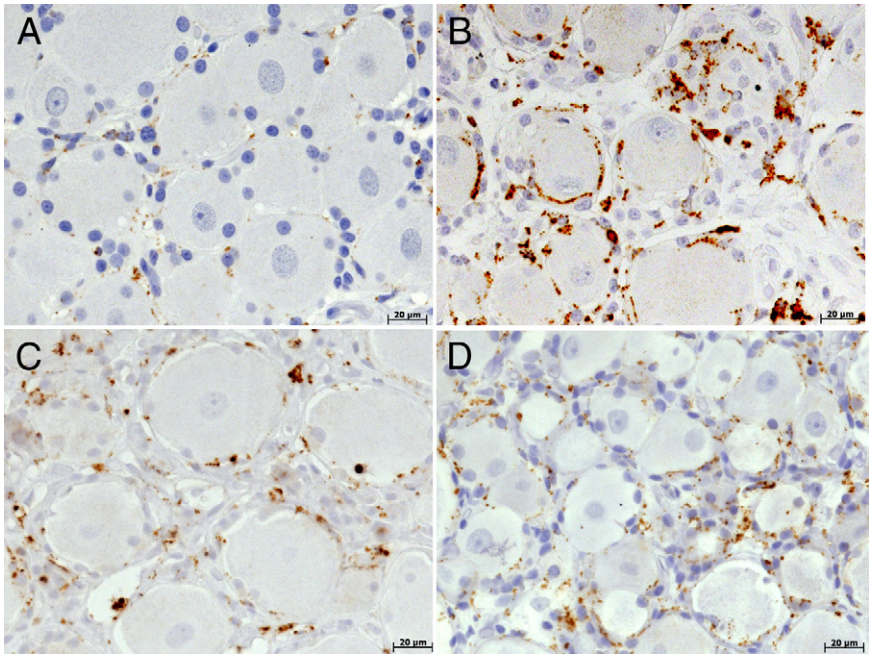

Figure 2. Elevated numbers and activation of $CD68^+$ macrophages in the DRG of a CD8-depleted SIV-infected macaque. To characterize the degree of satellitosis and macrophage activation in the CD8-depleted SIV-infected animals, sections of DRG tissues were immunostained with an anti-CD68 monoclonal antibody. **A:** A tissue section from a representative uninfected rhesus macaque (M2) DRG with CD68 immunoreactivity identifies a resident macrophage population diffusely around the DRG neurons. **B:** A representative section of DRG tissue from a CD8-depleted SIV-infected rhesus macaque (M6) demonstrates prominent cell processes and increased CD68 reactivity. **C:** Representative section of DRG tissue from a non-CD8-depleted SIV-infected rhesus macaque that was a rapid progressor (M10) with increased CD68 immune reactivity, compared with control. **D:** Representative section of DRG tissue from a non-CD8-depleted conventional progressor SIV-infected rhesus macaque (M13) with a moderate increase in CD68 reactivity, compared with control. Scale bars: 20 μm.

DRG tissues, consistent with increased reactivity (Figure 2B). In the non-CD8-depleted uninfected controls, the proportion of $CD68^+$ satellite cells ranged from 11.8% to 15.4% of total satellite cells; absolute numbers ranged from 420.6 to 569.7 $CD68^+$ satellite cells/mm^2 of DRG tissue (Table 1). The CD68 immunostaining in the non-CD8-depleted SIV-infected groups was more variable between animals, but both the overall percentage of $CD68^+$ satellite cells and the absolute number of $CD68^+$ cells in the DRG tissue were elevated, compared with uninfected animals (Table 1 and Figure 2, C and D).

DRG tissue was stained with an anti-SIV p28 antibody to analyze the number of productively SIV-infected satellite cells and to determine whether productive infection correlated with DRG pathology (Figure 3). Within the CD8-depleted SIV-infected animals SIV $p28^+$ cells ranged from 1.2% to 8.2%; absolute numbers of SIV $p28^+$ satellite cells ranged from 60.1 to 317.4 cells/mm^2 of DRG tissue (Table 1). In these animals, productively infected cells were consistently localized to ganglionic lesions of infiltrating cells and prominent neuronophagia (Figure 3A). In non-CD8-depleted SIV-infected animals with rapid disease progression, cells staining positively for SIV p28 ranged from 4.8% to 45.6%; absolute numbers of SIV $p28^+$ satellite cells ranged from 143.5 to 1921.8 cells/mm^2 of DRG tissue (Table 1 and Figure 3B). In contrast, there were few productively infected satellite cells in the non-CD8-depleted SIV-infected animals that were conventional progressors (2.0% to 2.6% of satellite cells and the absolute number of cells ranging from 70.0 to 127.1 cells/mm^2 of DRG tissue staining positively for SIV p28) (Table 1 and Figure 3C).

To examine the presence of T cells in DRG tissue and their possible role in DRG inflammation or in controlling SIV replication, sections of DRG tissue were immunostained with an anti-CD3 antibody. In the two CD8-depleted uninfected animals, the basal level of $CD3^+$ T cells in the DRG tissue was 101.1 and 191.2 cells/mm^2, with 2.6% to 6.4% of the satellite cells expressing CD3 (Table 1). In the SIV-infected CD8-depleted animals, the number

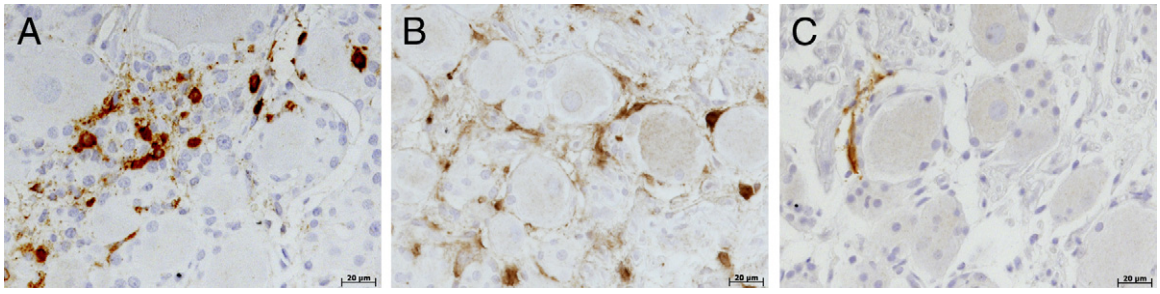

Figure 3. Abundant productive viral replication in DRG of SIV-infected macaques. IHC was performed on DRG tissue sections using an anti-SIV p28 antibody to identify productive replication within the DRG satellite cells. **A:** Representative section of DRG tissue from a CD8-depleted SIV-infected rhesus macaque (M6) with productively infected cells that were consistently localized to ganglionic lesions of infiltrating cells and prominent neuronophagia. **B:** A representative section of DRG tissue from a non-CD8-depleted SIV-infected rapid progressor rhesus macaque (M11) that progressed to AIDS within 6 months demonstrates abundant SIV p28 immunoreactivity. **C:** A representative section of DRG tissue from a non-CD8-depleted conventional progressor SIV-infected rhesus macaque (M14) shows very little productive infection in the satellite cells. Scale bars: 20 μm.

of $CD3^+$ T cells in the DRG tissues was not elevated, compared with uninfected controls. The percentage of $CD3^+$ T cells of total satellite cells ranged from 1.7% to 7.4% and the absolute number ranged from 96.3 to 252.6 $CD3^+$ cells/mm^2 of DRG tissue (Table 1). In the non-CD8-depleted uninfected animals, the basal number of $CD3^+$ T cells in the DRG tissue was slightly higher than the CD8-depleted animals, ranging from 293.5 to 597.6 cells/mm^2, with 7.0% to 11.2% of the satellite cells expressing CD3 (Table 1). In the SIV-infected CD8-depleted animals, the quantity of $CD3^+$ T cells in the DRG tissues was not significantly elevated in the rapid progressors, compared with non-CD8-depleted uninfected animals. The percentage of $CD3^+$ T cells in the total satellite cells in the conventional progressors was higher than in the uninfected animals, ranging from 5.3% to 19.3%; the absolute number ranged from 243.2 to 778.0 $CD3^+$ cells/mm^2 of DRG tissue (Table 1).

To assess the possible role or roles that $CD8^+$ T cells may have in either controlling SIV replication or in promoting inflammatory response in DRG tissue during SIV peripheral neuropathy, we examined the number of $CD8^+$ T cells present in the DRG tissue. In the CD8-depleted animals, both uninfected and infected, there was a similar range (0.0% to 6.2%) of total satellite cells that were $CD8^+$ (Table 1). There were more $CD8^+$ cells in DRG of the non-CD8-depleted animals (5.1% to 17.8% of total satellite cells), with the greatest number in the conventional progressors (Table 1).

Correlations

We found a positive correlation between the degree of DRG histopathology and the number of activated $CD68^+$ macrophages. Of the four CD8-depleted SIV-infected animals, M6 had the most severe pathology and the greatest percentage of $CD68^+$ satellite cells (severe DRG pathology with 28.1% $CD68^+$ satellite cells). M7 and M8 had moderate to severe DRG damage, with 26.1% and 24.4% $CD68^+$ satellite cells, respectively. M9 had moderate DRG pathology, with 19.1% $CD68^+$ satellite cells. Of the six animals in the non-CD8-depleted SIV-infected groups, those with mild DRG damage (M12, M14, and M15) had lower percentages of $CD68^+$ satellite cells (16.1% $\pm$ 0.8, 19.6% $\pm$ 1.4, and 10.6% $\pm$ 0.3, respectively) than those with moderate DRG pathology (M10, M11, and M13; 38.0% $\pm$ 1.6, 27.3% $\pm$ 3.2, and 24.5% $\pm$ 1.2, respectively) (Table 1). This trend did not hold true across all animals. Overall, CD8-depleted SIV-infected animals had the most severe pathology, but not the highest percentage of $CD68^+$ satellite cells.

To determine whether there is an accumulation of satellite cells around DRG neurons, total satellite cells were counted in H&E-stained sections; this total was divided by the number of neurons per section of tissue. In the uninfected control animals, the number of satellite cells ranged from 10.3 to 13.8 cells per DRG neuronal body (Table 1). Only two animals, both of them CD8-depleted SIV-infected, had a significantly increased number of satellite cells, compared with uninfected animals, with 26.0 $\pm$ 1.2 and 23.1 $\pm$ 1.5 cells per DRG neuronal body. BrdU labeling showed that $<$1% of the satellite cells in CD8-depleted uninfected animals were $BrdU^+$, whereas in CD8-depleted SIV-infected animals the percentage of $BrdU^+$ satellite cells ranged from 1.5% to 5% 24 hours after the BrdU bolus (data not shown). These data demonstrate that, in this model, macrophages traffic from bone marrow and accumulate around the DRG neurons within 24 hours after the BrdU bolus, which is increased during SIV-SN.

Discussion

With the present study, we have developed and characterized a CD8-depleted SIV-infected rhesus macaque model of SIV-SN. Using this model, we found that satellite cell activation and recruitment are critical components of DRG pathology. This rapid-progression model accurately resembles the peripheral nerve pathology evidenced in non-CD8-depleted SIV-infected animals with AIDS, but results in a higher incidence of SIV encephalitis in the CNS and more severe DRG pathogenesis. It is therefore an accurate and valuable model for elucidating the pathogenic mechanism or mechanisms of HIV-SN and consequent future treatment modalities.

In HIV infection, DRG are a site of neuronal damage, which is associated with reactive mononuclear phagocytes and HIV-infected macrophages. Increasingly, reports from human studies highlight the possible contribution of satellite cell activation and dorsal root inflammation to the persistence of pathological pain in peripheral neuropathy via activation of the sensory pathways that propagate peripheral signals back into the spinal cord and brain.[30,31] Our observations of morphological and IHC alterations in satellite cells within the DRG of SIV-infected CD8-depleted macaques recapitulates lesions of sensory neuropathy in a shorter time frame of AIDS progression: 3 to 4 months in CD8-depleted macaques, compared with $>$10 years in humans and $>$1 year in conventional progressor nondepleted macaques. Moderate to severe DRG pathology was found in the SIV-infected CD8-depleted macaques, which was characterized by abundant infiltration of mononuclear cells and subsequent formation of Nageotte nodules, thus substantiating the observation that neuronal loss occurs in the DRG of SIV-infected macaques. Consistent with these data, another report described trigeminal ganglionitis with neuronal loss and neuronophagia in SIV-infected pigtail macaques.[19]

An endogenous resident population of scattered $CD68^+$ macrophages is located within tissue of uninfected animals and is unchanged by CD8 T cell depletion itself in the absence of SIV infection. In infected animals, $CD68^+$ macrophages increased in number, surrounded neuronal bodies, and accumulated in distinct foci (rather than being dispersed evenly throughout the tissue), suggesting a role for activated satellite cells in perhaps initiating neuronophagia. These activated cells exhibited more prominent cell processes and extensive contact

with the DRG, indicating increased reactivity and enhanced phagocytic function. The phagocytic activation of macrophages presumably occurs in an attempt to combat the underlying viral infection and to clear degenerate neuronal residue.

The DRG pathology observed in the CD8-depleted animals was more severe than in the non-CD8-depleted SIV-infected animals, as measured by satellitosis and frequency of neuronophagia, whether the animals were conventional or rapid progressors, suggesting that $CD8^+$ T cells may play a role in protecting DRG neurons from damage. However, $CD8^+$ T cell numbers were elevated in the DRG only of the conventional progressors, and numbers in the rapid progressors were similar to those in the CD8-depleted animals, indicating that the $CD8^+$ T cells are not likely to be solely responsible for protecting the DRG neurons from damage. In addition, for examining the number of $CD3^+$ T cells and subtracting the number of $CD8^+$ T cells, we predict that the few remaining cells are likely to be $CD4^+$ T cells in the DRG. (CD4 IHC is not reliable in rhesus macaque paraffin tissue sections, because of low antigenicity, so we used a pan-T-cell marker against CD3.) The non-CD8-depleted animals with mild to moderate peripheral neuropathy generally had more productively infected satellite cells, compared with the CD8-depleted SIV-infected animals, including M6 (with severe DRG pathology), supporting the idea that productive infection of satellite cells is not a prerequisite nor is directly related to DRG damage. Of note, both of the non-CD8-depleted animals with the highest numbers of productively infected satellite cells were rapid progressors, so increased productive infection cannot be explained by a longer time progression to AIDS but may be explained in terms of the quantity of CD8 cells. The greatest numbers of $CD8^+$ T cells were found in the animals with the lowest numbers of productively infected cells.

To compare only peripheral effects of SIV infection with known CNS pathology, we selected animals that developed SIV encephalitis. As common as multinucleated giant cells are to CNS pathology in SIV encephalitis, we found no multinucleated giant cells present in the sensory ganglia examined from the same animals. Although similarities exist between the CNS and PNS with regard to SIV-associated pathologies, there are likely fundamental differences between the pathogenic mechanisms in the two affected areas, due in part to differences between the blood-brain barrier of the CNS and the blood-neural barrier of the PNS, as well as to the capacity of PNS neurons (but not CNS neurons) for extensive regeneration.

We conclude that with a more rapid progression to AIDS and typically a higher severity of peripheral neuropathy, the CD8-depleted SIV-infected rhesus macaque can serve as a valuable model for studying the pathogenesis of HIV-induced PNS disease. In this model, activation of endogenous $CD68^+$ macrophages plays substantial roles in perpetuating DRG damage and neuronal loss, as characterized by frequent neuronophagia and formation of Nageotte nodules.

Acknowledgments

We thank Drs. Andrew A. Lackner, Ronald S. Veazey, and Patricia E. Molina for the use of non-CD8-depleted SIV-infected DRG tissues, Dr. Peter J. Didier for collection of retrospective DRG tissues from the non-CD8-depleted SIV-infected animals, Cecily Conerly Midkiff and Dr. Xavier Alvarez for assistance in obtaining uninfected non-CD8-depleted tissues, the veterinary staff at both the New England Primate Research Center and the Tulane National Primate Research Center for animal care, and pathology residents and staff for assisting with necropsies and tissue collection.

References

1. Autran B, Carcelain G, Li TS, Blanc C, Mathez D, Tubiana R, Katlama C, Debre P, Leibowitch J: Positive effects of combined antiretroviral therapy on CD4+ T cell homeostasis and function in advanced HIV disease. Science 1997, 277:112–116
2. Brinley FJ Jr, Pardo CA, Verma A: Human immunodeficiency virus and the peripheral nervous system workshop. Arch Neurol 2001, 58:1561–1566
3. Manji H: Neuropathy in HIV infection. Curr Opin Neurol 2000, 13:589–592
4. Verma A: Epidemiology and clinical features of HIV-1 associated neuropathies. J Peripher Nerv Syst 2001, 6:8–13
5. Zhu Y, Jones G, Tsutsui S, Opii W, Liu S, Silva C, Butterfield DA, Power C: Lentivirus infection causes neuroinflammation and neuronal injury in dorsal root ganglia: pathogenic effects of STAT-1 and inducible nitric oxide synthase. J Immunol 2005, 175:1118–1126
6. Letendre SL, Ellis RJ, Everall I, Ances B, Bharti A, McCutchan JA: Neurologic complications of HIV disease and their treatment. Top HIV Med 2009, 17:46–56
7. Wulff EA, Wang AK, Simpson DM: HIV-associated peripheral neuropathy: epidemiology, pathophysiology and treatment. Drugs 2000, 59:1251–1260
8. Ellis RJ, Marquie-Beck J, Delaney P, Alexander T, Clifford DB, McArthur JC, Simpson DM, Ake C, Collier AC, Gelman BB, McCutchan JA, Morgello S, Grant I; CHARTER Group: Human immunodeficiency virus protease inhibitors and risk for peripheral neuropathy. Ann Neurol 2008, 64:566–572
9. Bhangoo SK, Ripsch MS, Buchanan DJ, Miller RJ, White FA: Increased chemokine signaling in a model of HIV1-associated peripheral neuropathy. Mol Pain 2009, 5:48
10. Keswani SC, Jack C, Zhou C, Hoke A: Establishment of a rodent model of HIV-associated sensory neuropathy. J Neurosci 2006, 26:10299–10304
11. Kennedy JM, Hoke A, Zhu Y, Johnston JB, van Marle G, Silva C, Zochodne DW, Power C: Peripheral neuropathy in lentivirus infection: evidence of inflammation and axonal injury. AIDS 2004, 18:1241–1250
12. Zhu Y, Antony JM, Martinez JA, Glerum DM, Brussee V, Hoke A, Zochodne D, Power C: Didanosine causes sensory neuropathy in an HIV/AIDS animal model: impaired mitochondrial and neurotrophic factor gene expression. Brain 2007, 130:2011–2023
13. Desrosiers RC: The simian immunodeficiency viruses. Annu Rev Immunol 1990, 8:557–578
14. Lackner AA: Pathology of simian immunodeficiency virus induced disease. Curr Top Microbiol Immunol 1994, 188:35–64
15. Sasseville VG, Lackner AA: Neuropathogenesis of simian immunodeficiency virus infection in macaque monkeys. J Neurovirol 1997, 3:1–9
16. Westmoreland SV, Halpern E, Lackner AA: Simian immunodeficiency virus encephalitis in rhesus macaques is associated with rapid disease progression. J Neurovirol 1998, 4:260–268
17. Williams KC, Hickey WF: Central nervous system damage, monocytes and macrophages, and neurological disorders in AIDS. Annu Rev Neurosci 2002, 25:537–562

18. Lackner AA, Dandekar S, Gardner MB: Neurobiology of simian and feline immunodeficiency virus infections. Brain Pathol 1991, 1:201–212
19. Laast VA, Pardo CA, Tarwater PM, Queen SE, Reinhart TA, Ghosh M, Adams RJ, Zink MC, Mankowski JL: Pathogenesis of simian immunodeficiency virus-induced alterations in macaque trigeminal ganglia. J Neuropathol Exp Neurol 2007, 66:26–34
20. Jin X, Bauer DE, Tuttleton SE, Lewin S, Gettie A, Blanchard J, Irwin CE, Safrit JT, Mittler J, Weinberger L, Kostrikis LG, Zhang L, Perelson AS, Ho DD: Dramatic rise in plasma viremia after CD8(+) T cell depletion in simian immunodeficiency virus-infected macaques. J Exp Med 1999, 189:991–998
21. Madden LJ, Zandonatti MA, Flynn CT, Taffe MA, Marcondes MC, Schmitz JE, Reimann KA, Henriksen SJ, Fox HS: CD8+ cell depletion amplifies the acute retroviral syndrome. J Neurovirol 2004, 10 Suppl 1:58–66
22. Matano T, Shibata R, Siemon C, Connors M, Lane HC, Martin MA: Administration of an anti-CD8 monoclonal antibody interferes with the clearance of chimeric simian/human immunodeficiency virus during primary infections of rhesus macaques. J Virol 1998, 72:164–169
23. Metzner KJ, Jin X, Lee FV, Gettie A, Bauer DE, Di Mascio M, Perelson AS, Marx PA, Ho DD, Kostrikis LG, Connor RI: Effects of in vivo CD8(+) T cell depletion on virus replication in rhesus macaques immunized with a live, attenuated simian immunodeficiency virus vaccine. J Exp Med 2000, 191:1921–1931
24. Roberts ES, Zandonatti MA, Watry DD, Madden LJ, Henriksen SJ, Taffe MA, Fox HS: Induction of pathogenic sets of genes in macrophages and neurons in NeuroAIDS. Am J Pathol 2003, 162:2041–2057
25. Schmitz JE, Johnson RP, McClure HM, Manson KH, Wyand MS, Kuroda MJ, Lifton MA, Khunkhun RS, McEvers KJ, Gillis J, Piatak M, Lifson JD, Grosschupff G, Racz P, Tenner-Racz K, Rieber EP, Kuus-Reichel K, Gelman RS, Letvin NL, Montefiori DC, Ruprecht RM, Desrosiers RC, Reimann KA: Effect of CD8+ lymphocyte depletion on virus containment after simian immunodeficiency virus SIVmac251 challenge of live attenuated SIVmac239delta3-vaccinated rhesus macaques. J Virol 2005, 79:8131–8141
26. Schmitz JE, Kuroda MJ, Santra S, Sasseville VG, Simon MA, Lifton MA, Racz P, Tenner-Racz K, Dalesandro M, Scallon BJ, Ghrayeb J, Forman MA, Montefiori DC, Rieber EP, Letvin NL, Reimann KA: Control of viremia in simian immunodeficiency virus infection by CD8+ lymphocytes. Science 1999, 283:857–860
27. Schmitz JE, Simon MA, Kuroda MJ, Lifton MA, Ollert MW, Vogel CW, Racz P, Tenner-Racz K, Scallon BJ, Dalesandro M, Ghrayeb J, Rieber EP, Sasseville VG, Reimann KA: A nonhuman primate model for the selective elimination of CD8+ lymphocytes using a mouse-human chimeric monoclonal antibody. Am J Pathol 1999, 154:1923–1932
28. Williams K, Westmoreland S, Greco J, Ratai E, Lentz M, Kim WK, Fuller RA, Kim JP, Autissier P, Sehgal PK, Schinazi RF, Bischofberger N, Piatak M, Lifson JD, Masliah E, Gonzalez RG: Magnetic resonance spectroscopy reveals that activated monocytes contribute to neuronal injury in SIV neuroAIDS. J Clin Invest 2005, 115:2534–2545
29. Nath A: Pathobiology of human immunodeficiency virus dementia. Semin Neurol 1999, 19:113–127
30. Hanani M: Satellite glial cells in sensory ganglia: from form to function. Brain Res Brain Res Rev 2005, 48:457–476
31. Takeda M, Takahashi M, Matsumoto S: Contribution of the activation of satellite glia in sensory ganglia to pathological pain. Neurosci Biobehav Rev 2009, 33:784–792